Journal of Quantitative Spectroscopy & Radiative Transfer 165 (2015) 22–27

Contents lists available at ScienceDirect

Journal of Quantitative Spectroscopy & Radiative Transfer

journal homepage: www.elsevier.com/locate/jqsrt

Cavity ring-down spectroscopy of CO_2 overtone bands near 830 nm

Y. Tan [a], X.-Q. Zhao [a], A.-W. Liu [a,b,*], S.-M. Hu [a], O.M. Lyulin [c], S.A. Tashkun [c,d], V.I. Perevalov [c]

[a] Hefei National Laboratory for Physical Sciences at Microscale, iChem Center, University of Science and Technology of China, Hefei 230026, China
[b] Synergetic Innovation Center of Quantum Information & Quantum Physics, University of Science and Technology of China, Hefei 230026, China
[c] Laboratory of Theoretical Spectroscopy, V. E. Zuev Institute of Atmospheric Optics, Siberian Branch, Russian Academy of Sciences, 1, Academician Zuev sq., 634021 Tomsk, Russia
[d] Tomsk State University, Laboratory of Quantum Mechanics of Molecules and Radiative Processes, Lenin av. 36, 634050 Tomsk, Russia

ARTICLE INFO

Article history:
Received 12 April 2015
Received in revised form
10 June 2015
Accepted 11 June 2015
Available online 19 June 2015

Keywords:
Carbon dioxide
Cavity ring down spectroscopy
Vibration–rotation
Line positions
Line intensities
Effective dipole moment parameters

ABSTRACT

Three bands 4003*i*–00001 (i=2, 3, 4) of the Fermi pentad of $^{12}C^{16}O_2$ near 830 nm have been recorded with a continuous-wave cavity ring down spectrometer. A sensitivity at the 5×10^{-11} cm^{-1} level allowed us to obtain line positions and intensities of these very weak bands. The measured line intensities of these three bands together with those published for the 10051–00001 and 10052–00001 bands were used to obtain the effective dipole moment parameters of $^{12}C^{16}O_2$ for the ΔP=17 series of transitions, where $P=2V_1+V_2+3V_3$ is a polyad number (V_i (i=1, 2, 3) are vibrational quantum numbers). Comparisons of the measured line positions and intensities of the 4003*i*–00001 (i=2, 3, 4) bands to those from the AMES and GEISA line lists are given.

1. Introduction

Carbon dioxide is one of the most important greenhouse gases and a major species of the atmospheres of some rocky planets. It has many vibrational bands with very different intensities from the far infrared to visible region, which makes it possible to monitor the evolution of carbon dioxide in Earth's atmosphere, and probe other atmospheres to different depths. The vibrational bands in the near-infrared region of CO_2 are strong enough to be easily detected without saturation due to the absorption of the atmospheres of Venus [1] and Mars [2]. The relatively strong bands of $^{12}C^{16}O_2$ around 870 nm and 782 nm have been studied by many groups [3–6] with high accuracy. While the relative weak bands 4003*i*–00001 (i=1, 2, 3, 4, 5) of the Fermi pentad of $^{12}C^{16}O_2$ near 830 nm have never been quantitatively studied. Only the band-heads of the three strongest bands of this Fermi pentad were observed with photo-acoustic spectroscopy [7]. The calculated line parameters of these bands are included in the latest GEISA database [8] and AMES line list [9]. According to the theoretical prediction, the rotational structures of the three strongest bands 4003*i*–00001 (i=2, 3, 4) of the Fermi pentad could be measured with our cavity ring down spectrometer.

The present work is the continuation of a series devoted to the systematic study of the absorption spectrum of isotopologues of carbon dioxide above 1 μm in our laboratory [6,10–11]. In this paper, the study of the

* Corresponding author at: Synergetic Innovation Center for Quantum Information & Quantum Physics, University of Science and Technology of China, Hefei 230026, China. Tel.: +86 551 63607632.
E-mail address: awliu@ustc.edu.cn (A.-W. Liu).

http://dx.doi.org/10.1016/j.jqsrt.2015.06.010
0022-4073/

4003*i*–00001 bands of the Fermi pentad will be presented. The measured line positions and intensities can be used to refine the effective Hamiltonian and dipole moment parameters for the $^{12}C^{16}O_2$ isotopologue.

2. Experimental details

The configuration of the continuous-wave (CW) cavity ring-down spectrometer based on a Ti:Sapphire laser has been described in detail in Ref. [12]. Briefly, the structure of the setup is as follows: a beam from a CW tunable Ti: sapphire laser (Coherent MBR 110) is coupled into a 65.5-cm-long resonance cavity. Cavity mirrors (Layertec GmbH) with a reflectivity of 99.995% are installed in a high-vacuum chamber and can be precisely adjusted by a set of step-motors (New Focus Picomotor) using a controller outside the chamber. The ring-down signal is detected by a photodiode and recorded by an analog-digital converter (ADLink PCI 9228) installed on a personal computer. A nonlinear least-square fitting program is applied to fit the data to derive the ring-down time τ. The sample absorption coefficient α at frequency ν is obtained from the equation:

$$\alpha(\nu)=\frac{1}{c\tau(\nu)}-\frac{1}{c\tau_0} \tag{1}$$

where c is the speed of light and τ_0 is the ring-down time of the empty cavity. The typical noise-equivalent absorption coefficient is 5×10^{-11} cm^{-1}.

Natural carbon dioxide gas with a stated purity of 99.99% was bought from the Nanjing Special Gas Co. and further purified by a "freeze–pump–thaw" process before use. Two pressures of 48.5 and 50.9 kPa were adopted and the spectrum was recorded at room temperature (296 K). The sample pressure was measured by a capacitance gauge (Shanghai ZhenTai CPCA-140Z; full range 100 kPa) with a stated accuracy of 0.5%. The spectrum calibration was based on the readings given by a calibrated lambda-meter (Burleigh WA-1500) with 60 MHz accuracy.

Since the 4003*i*–00001 (i=2,3,4) bands of $^{12}C^{16}O_2$ are located in a spectral region with strong water absorption lines, the CO_2 absorption transitions were recorded line-by-line according to the theoretical calculation of AMES [9].

3. Results

3.1. Transition list

The spectral line parameters were retrieved by fitting the observed spectra. The line shape was modeled by a Voigt profile in which the Doppler line width was fixed at the calculated value. The adjustable parameters include position, intensity, line width, and the parameters for the baseline which are modeled by a second order polynomial. We had to take into account the baseline because practically all lines are blended with stronger water lines. We estimate that the CO_2 sample contains about 0.01% of water, which comes as an impurity of the sample gas and also from degassing of the ring-down cavity. The apparatus function was not taken into account because the line width of the laser is much smaller than the spectral line widths. As an example, in Fig. 1, we present the observed and simulated profiles of the P18 line in the 40033–00001 band. The residuals of the fit are also presented in this figure.

A total of 77 $^{12}C^{16}O_2$ transitions were observed. The full line list is presented in Table 1. The values of the line strength in the table have been converted to 100% abundance of $^{12}C^{16}O_2$. The uncertainty in the line positions varies from 0.002 cm^{-1} to 0.030 cm^{-1}, while the uncertainty in the line intensities is about 5% for strong and well-isolated lines, but up to 100% for very weak or heavily blended lines.

3.2. Spectroscopic constants of the upper states

Three vibrational bands were rotationally identified according to the AMES line list [9]. The rotational analysis was performed using the standard equation for the vibration–rotation energy levels:

$$F_v(J)=G_v+B_vJ(J+1)-D_vJ^2(J+1)^2+H_vJ^3(J+1)^3, \tag{2}$$

where G_v is the vibrational term value, B_v is the rotational constant, D_v and H_v are centrifugal distortion constants, and J is the angular momentum quantum number. The spectroscopic parameters for an upper state were fitted directly to the observed line positions of the respective band. The ground state rotational constants were constrained to the literature values [14]. The spectroscopic parameters of the 4003*i* (i=2, 3, 4) states retrieved from the fit are presented in Table 2.

3.3. Effective dipole moment parameters

Using the line intensities for the 4003*i*–00001 (i=2,3,4) bands measured in this work and those recently published [6,10] for the 1005*i*–00001 (i=1, 2) and 1115*i*–01101

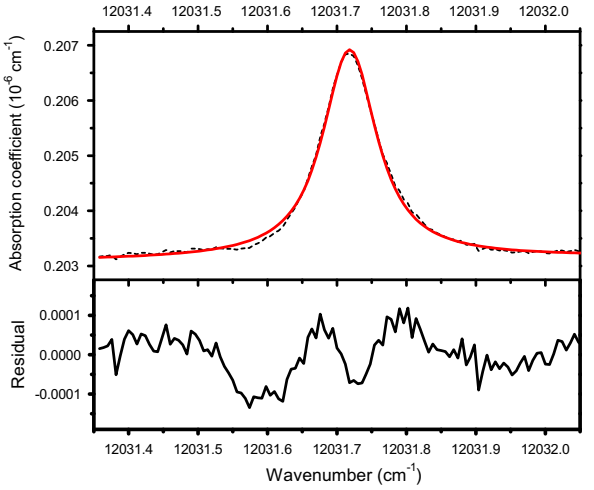

Fig. 1. The P18 line of the 40033–00001 band of $^{12}C^{16}O_2$ recorded at room temperature and at 0.478 atm pressure. The dashed line represents the observed line and the straight line represents the simulated line. The residuals are given on the below panel.

Table1
Line parameters of the 4003*i*–00001 (i=2, 3, 4) bands of $^{12}C^{16}O_2$.

Line	Position (cm^{-1})	Intensity (10^{-30} cm/molecule)	Position (cm^{-1})	Intensity (10^{-30} cm/molecule)	Position (cm^{-1})	Intensity (10^{-30} cm/molecule)
	40032–00001		**40033–00001**		**40034–00001**	
P 38					11,870.814 [a]	3.0
P 36			12,008.970	20.1	11,873.638[a]	7.7
P 34	12,142.936[b]	6.8	12,011.710	20.9	11,876.385[a]	5.3
P 32					11,879.058[a]	8.6
P 30	12,148.400[b]	5.6	12,017.067	30.9	11,881.657[b]	9.3
P 28	12,151.025[b]	5.7	12,019.671	31.0	11,884.184[b]	7.6
P 26			12,022.204	44.0	11,886.653	20.2
P 22	12,158.451	19.0	12,027.101[b]	26.4	11,891.372	16.8
P 20	12,160.785[b]	10.7	12,029.441	42.5	11,893.631[b]	20.9
P 18	12,163.038[b]	22.6	12,031.715	46.5		
P 16			12,033.888[b]		11,897.934	16.7
P 14	12,167.330	16.8	12,036.031	51.2		
P 12			12,038.079[b]	19.4	11,901.964	16.3
P 10					11,903.882[b]	12.5
P 8	12,173.207[b]	23.8	12,041.941	41.1		
P 6			12,043.750	10.2	11,907.501[b]	13.2
P 4	12,176.749[c]	4.0	12,045.495	13.0		
P 2			12,047.155[a]	4.5		
R 0	12,180.708 [c]	4.3	12,049.488[a]	6.6		
R 2	12,182.199[b]	11.9	12,050.953[a]	2.6		
R 4	12,183.584[a]	8.1	12,052.338[a]	16.2	11,916.091[a]	4.0
R 6	12,184.911[a]	7.6	12,053.648[a]	6.9	11,917.449[a]	8.1
R 8	12,186.144[b]	16.0	12,054.874	46.7	11,918.696	18.8
R 10	12,187.311[b]	23.6			11,919.917	17.0
R 12	12,188.395[b]	21.3	12,057.099	57.4		
R 14			12,058.098	62.3		
R 16	12,190.341[a]	15.9	12,059.026	68.1	11,923.120[b]	17.8
R 18	12,191.228[a]	23.9	12,059.868[a]	9.1		
R 20	12,192.010[a]	14.2	12,060.650	51.3	11,924.921[b]	8.7
R 22	12,192.717	9.6	12,061.356	48.8	11,925.713[b]	6.7
R 24					11,926.439	12.9
R 26	12,193.932[b]	18.6			11,927.093	11.9
R 28	12,194.423[a]	11.7	12,063.082[b]	38.6	11,927.675	12.5
R 30					11,928.188	12.2
R 32			12,063.961	21.4	11,928.630[b]	10.0
R 34					11,929.005[a]	2.7
R 36			12,064.666	14.3		

Note: For an unblended line the uncertainty of the line position is 0.002–0.005 cm^{-1} and the uncertainty of the line intensity is 5–10%.
[a] For a strongly blended line the uncertainty of the line position is 0.01–0.02 cm^{-1} and the uncertainty of the line intensity is 30–50%.
[b] For a blended line the uncertainty of the line position is 0.005–0.010 cm^{-1} and the uncertainty of the line intensity is 20–30%.
[c] For a very weak line the uncertainty of the line position is 0.02–0.03 cm^{-1} and the uncertainty of the line intensity is 50–100%.

Table 2
Spectroscopic constants (in cm^{-1}) of the 4003*i* (i=2, 3, 4) vibrational states of $^{12}C^{16}O_2$.

Ground state	G_v	B_v	$D_v \times 10^7$	$H_v \times 10^{10}$		
00001	0.00000	0.39021894	1.334088	1.918	Ref.[14]	
Upper state	G_v	B_v	$D_v \times 10^7$	$H_v \times 10^{10}$	*RMS*[a]	n/N[b]
40032	12,179.9669(20)	0.380781(12)	0.74(13)	1.918[c]	3.6	18/22
40033	12,048.7317(13)	0.3804269(91)	−0.46(16)	1.798(78)	2.9	28/29
40034	11,912.4363(43)	0.381869(35)	3.37(66)	0.69(35)	3.9	24/26

[a] RMS – root mean squares of residuals in 10^{-3} cm^{-1}.
[b] n, number of transitions included in the fit; N, number of assigned rotational transitions.
[c] This parameter was fixed at the value of the ground state in the rotational analysis.

(i=1, 2) bands, we have performed fits to obtain the effective dipole moment parameters for the ΔP=17 series of transitions. The line intensity is proportional to the transition dipole moment squared which, within the framework of the effective operators approach, is given by the following equation [15–17]:

In this equation ${}^{J}C_{PN\varepsilon}^{V_1V_2l_2V_3}$ and ${}^{J'}C_{P'N'\varepsilon'}^{V_1+\Delta V_1V_2+\Delta V_2l_2+\Delta l_2V_3+\Delta V_3}$ are the expansion coefficients

$$W_{P'N'J'\varepsilon'\leftarrow PNJ\varepsilon}=(2J+1)\left|\sum_{\substack{2V_1+V_2+3V_3=P\\ \ell_2}}\sum_{\substack{2\Delta V_1+\Delta V_2+3\Delta V_3=\Delta P\\ \Delta\ell_2=0,\pm1,\pm2,\ldots}}{}^{J}C_{PN\varepsilon}^{V_1V_2\ell_2V_3J'}C_{P'N'\varepsilon'}^{V_1+\Delta V_1V_2+\Delta V_2\ell_2+\Delta\ell_2V_3+\Delta V_3}M_{\Delta V}^{|\Delta\ell_2|}\right.$$
$$\left.\times\sqrt{f_{\Delta V}^{\Delta\ell_2}(V,\ell_2)\left(1+\delta_{\ell_2,0}+\delta_{\ell_2',0}-2\delta_{\ell_2,0}\delta_{\ell_2',0}\right)}\Phi_{\Delta J,\Delta\ell_2}(J,\ell_2)\right|^2 \quad (3)$$

of the eigenfunctions for lower and upper states, respectively, in the basis of harmonic oscillators and rigid symmetric top eigenfunctions, $\delta_{i,j}$ is the Kronecker symbol. The functions $f_{\Delta V}^{\Delta\ell_2}(V,\ell_2)$ are known functions of the vibrational quantum numbers. They are listed in Table 1 of Ref. [16] for small values of the quantum number differences ΔV. The functions $\Phi_{\Delta J\Delta\ell_2}(J,\ell_2)$ for $\Delta\ell_2=0,\ \pm1$ are equal to the Clebsh–Gordon coefficients $(1\Delta\ell_2 J\ell_2|(J+\Delta J)(\ell_2+\Delta\ell_2))$. We omit the Herman–Wallis type factors in this equation because they are not important in the present fit. The parameters $M_{\Delta V}^{\Delta\ell_2}$ of the matrix elements of the effective dipole moment operator are determined by the least squares fit to the observed line intensities. The computer code used for the fit is described in Ref. [18].

The purpose of the fit is to minimize the value of the dimensionless standard deviation, χ, defined as

$$\chi=\sqrt{\frac{\sum_{i=1}^{N}\left(\left(S_i^{obs}-S_i^{calc}\right)/\delta_i\right)^2}{N-n}}, \quad (4)$$

where S_i^{obs} and S_i^{calc} are, respectively, the observed and calculated values of the intensity for the ith line, $\delta_i=(S_i^{obs}\sigma_i)/100\%$ is the absolute measurement error of ith line, σ_i is the measurement error in percent, N is the number of fitted line intensities, and n is the number of adjusted effective dipole moment parameters. The measurement errors used in the present fit are given in Table 3. For the line intensities measured in the present work, the error varies from 5% to 50%. We used the eigenfunctions of the effective Hamiltonian published in Ref. [13]. The total internal partition function was taken from Ref. [19].

For the description of the quality of a fit we use also the value of the root mean square deviation defined by the

Table 4
Effective dipole moment parameters in 10^{-7} Debye for the $\Delta P=17$ series of transitions of $^{12}C^{16}O_2$.

Parameter	ΔV_1	ΔV_2	ΔV_3	$\Delta\ell_2$	Value
M	1	0	5	0	−4.6405 (49) [a]
M	0	2	5	0	0.1944 (27)
M	4	0	3	0	−0.5751 (71)

[a] The numbers in parentheses correspond to one standard deviation in units of the last quoted digit.

Table 3
Statistics of the line intensity fit.

Band	N	J_{min}	J_{max}	ν_{min}	ν_{max}	S_{min}	S_{max}	RMS (%)	Experimental uncertainty (%)	Reference
10051–00001	46	0	53	12,697.5	12,783.9	8.72E−29	3.32E−27	2.5	2	Song
10051–00001	33	0	50	12,697.5	12,783.6	1.18E−28	3.32E−27	1.7	1	Lu
10052–00001	32	2	52	12,592.9	12,682.2	4.68E−29	1.55E−27	2.7	2	Song
11151e–01101e	24	1	45	12,666.1	12,740.6	1.32E−29	1.12E−28	20.0	20	Song
11151f–01101f	25	2	45	12,672.5	12,740.4	1.14E−29	1.28E−28	19.2	20	Song
11152e–01101e	25	1	37	12,543.3	12,601.2	9.09E−30	9.61E−29	28.3	20	Song
11152f–01101f	26	2	41	12,545.4	12,601.4	8.91E−30	7.17E−29	23.2	20	Song
40032–00001	18	2	34	12,142.9	12,193.9	5.60E−30	4.66E−29	43.5	5–50	TW
40033–00001	23	0	36	12,009.0	12,064.7	4.50E−30	6.81E−29	31.7	5–50	TW
40034–00001	25	4	38	11,870.8	11,929.0	2.70E−30	2.09E−29	40.3	5–50	TW

Notes:
Ref.: TW – this work, Lu – Ref. [6], Song – Ref. [10].
N – number of fitted lines of a given band.
J_{min}, J_{max} – minimum and maximum values of the rotational quantum number J, respectively.
ν_{min}, ν_{max} – minimum and maximum values of the wavenumber of a given band, respectively.
S_{min}, S_{max} – minimum and maximum values of the line intensity of a given band, respectively.
RMS – root mean square of the residuals $(S_{obs}-S_{calc})/S_{obs}$ in percent (see Eq. (5)).

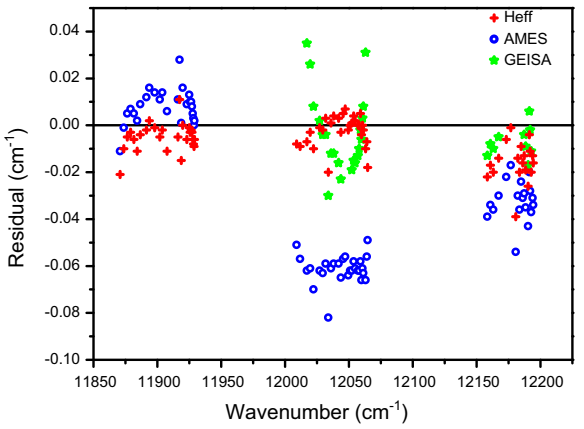

Fig. 2. Residuals between observed line positions and those from the AMES line list (open circles), from the GEISA database (open stars), and the line positions calculated with improved effective Hamiltonian (crosses).

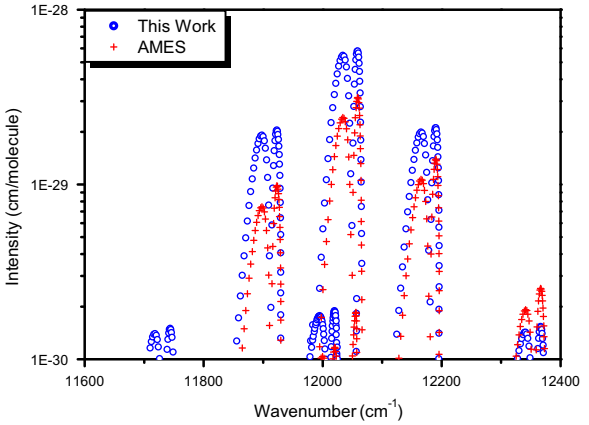

Fig. 3. Comparison of the line intensities of $^{12}C^{16}O_2$ for the $\Delta P=17$ series of transitions from the AMES line list (crosses), to the new line list generated with the new effective dipole moment parameters given in this work (open circles). (For interpretation of the references to color in this figure legend, the reader is referred to the web version of this article.)

equation:

$$RMS=\sqrt{\frac{\sum_{i=1}^{N}\left(\left(S_i^{obs}-S_i^{calc}\right)/S_i^{obs}\right)^2}{N}}\times 100\%. \quad (5)$$

The characteristics of the input data and the results of the fits are presented in Table 3. The fitted sets of the effective dipole moment parameters are given in Table 4.

4. Discussion and conclusion

In Fig. 2, we give a comparison of the line positions measured in this work to the values from the GEISA database [8] and those from the AMES line list [9]. The discrepancy in line positions between our measurement and those from the AMES line list for the 40033–00001 band reach 0.06 cm^{-1}. Meanwhile, the difference between the observed line positions and the values from the GEISA database varies from 0.025 to 0.04 cm^{-1}. This is because the GEISA database contains the line positions for 4003*i*–00001($i=2$, 3) bands from calculations using the effective Hamiltonian of Ref. [13]. It is obvious that the line position residual varies the square of the wavenumber for the 40033–00001 band. While the *rms* values (*obs.–calc.*) of the 40033–00001 band are found to be 2.9×10^{-3} cm^{-1} by fitting the observed line positions with the isolated vibrational state model, which is consistent with the experimental accuracy. It means that no perturbations could be identified within this experimental accuracy. The agreement between the observed and calculated values of the line positions could be improved if one takes into account additional anharmonic resonance term with the nonvanishing matrix element $\langle V_1V_2\ell_2V_3J|H^{eff}|V_1-1V_2-4\ell_2V_3+2J\rangle$ in the effective Hamiltonian. The respective residuals are also presented in Fig. 2 (H_{eff}). The newly observed line positions will allow us to improve the set of effective Hamiltonian parameters.

Although the uncertainties of the measured line intensities are estimated to vary from 5% to 100%, it is still instructive to compare them with those from the existing line lists. On average, they are two or three times larger than those from the AMES line list [9] and one order of magnitude larger than those from the GEISA database [8]. Using the new set of the effective dipole moment parameters, we generated a new line list of the $\Delta P=17$ series of transitions, which agree well with the measured values. This line list will be placed into a new version of the CDSD databank [20,21]. Meanwhile, we present the line intensity comparison between the AMES and the newly generated line list in the 11,600–12,400 cm^{-1} in Fig. 3. The line intensities for the 4003*i* ($i=1$, 2, 3, 4) bands generated in this work are two or three times larger than those from the AMES [9]. The calculated line intensities of the 40035 band obtained in this work are also stronger than those from the AMES [9], which should be confirmed by further experimental studies.

Acknowledgments

This work is jointly supported by the NSFC (21225314, 21303176, and 21473172) and RFBR (Russia, grant N 14-05-91150).

References

[1] Adel A. A determination of the amount of carbon dioxide above the reflecting layer in the atmosphere of the planet Venus. Astrophys J 1937;85:345–61.
[2] Spinrad H, Schorn RA, Moore R, Giver LP, Smith HJ. High-dispersion spectroscopic observations of Mars.1. CO_2 content and surface pressure. Astrophys J 1966;146:331.
[3] Yang XK, Petrillo CJ, Noda C. Photoacoustic detection of N_2O and CO_2 overtone transitions in the near-infrared. Chem Phys Lett 1993;214:536–40.
[4] Lucchesini A, Gozzini S. Diode laser overtone spectroscopy of CO_2 at 780 nm. J Quant Spectrosc Radiat Transf 2005;96:289–99.
[5] Campargue A, Bailly D, Teffo JL, Tashkun SA, Perevalov VI. The $\nu_1+5\nu_3$ dyad of $^{12}CO_2$ and $^{13}CO_2$. J Mol Spectrosc 1999;193:204–12.

[6] Lu Y, Liu AW, Li XF, Wang J, Cheng CF, Sun YR, et al. Line parameters of the 782 nm band of CO_2. Astrophys J 2013;775:71.
[7] Yang X, Noda C. Overtone transitions of $^{12}CO_2$ beyond the Venus bands. J Mol Spectrosc 1999;195:256–62.
[8] Jacquinet-Husson N, Crepeau L, Armante R, Boutammine C, Chedin A, Scott NA, et al. The 2009 edition of the GEISA spectroscopic database. J Quant Spectrosc Radiat Transf 2011;112:2395–445.
[9] Huang X, Gamache RR, Freedman RS, Schwenke DW, Lee TJ. Reliable infrared line lists for 13 CO_2 isotopologues up to $E'=18{,}000\ cm^{-1}$ and 1500 K with line shape parameters. J Quant Spectrosc Radiat Transf 2014;147:134–44.
[10] Song KF, Lu Y, Tan Y, Gao B, Liu AW, Hu SM. High sensitivity cavity ring down spectroscopy of CO_2 overtone bands near 790 nm. J Quant Spectrosc Radiat Transf 2011;112:761–8.
[11] Pan H, Li XF, Lu Y, Liu AW, Perevalov VI, Tashkun SA, et al. Cavity ring down spectroscopy of ^{18}O and ^{17}O enriched carbon dioxide near 795 nm. J Quant Spectrosc Radiat Transf 2013;114:42–4.
[12] Gao B, Jiang W, Liu AW, Lu Y, Cheng CF, Cheng GS, et al. Ultra sensitive near-infrared cavity ring down spectrometer for precise line profile measurement. Rev Sci Instrum 2010;81:043105.
[13] Majcherova Z, Macko P, Romanini D, Perevalov VI, Tashkun SA, Teffo JL, et al. High-sensitivity CW-cavity ring down spectroscopy of $^{12}CO_2$ near 1.5 μm. J Mol Spectrosc 2005;230:1–21.
[14] Miller CE, Brown LR. Near infrared spectroscopy of carbon dioxide I. $^{16}O^{12}C^{16}O$ line positions. J Mol Spectrosc 2004;228:329–54.
[15] Teffo JL, Sulakshina ON, Perevalov VI. Effective Hamiltonian for rovibrational energies and line intensities of carbon dioxide. J Mol Spectrosc 1992;156:48–64.
[16] Perevalov VI, Lobodenko EI, Lyulin OM, Teffo JL. Effective dipole moment and band intensities problem for carbon dioxide. J Mol Spectrosc 1995;171:435–52.
[17] Teffo JL, Lyulin OM, Perevalov VI, Lobodenko EI. Application of the effective operator approach to the calculation of $^{12}C^{16}O_2$ line intensities. J Mol Spectrosc 1998;187:28–41.
[18] Tashkun SA, Perevalov VI, Teffo JL, Tyuterev VG. Global fit of $^{12}C^{16}O_2$ vibrational–rotational line intensities using the effective operator approach. J Quant Spectrosc Radiat Transf 1999;62:571–98.
[19] Fischer J, Gamache RR, Goldman A, Rothman LS, Perrin A. Total internal partition sums for molecular species in the 2000 edition of the HITRAN database. J Quant Spectrosc Radiat Transf 2003;82:401–12.
[20] Perevalov VI, Tashkun SA. CDSD-296(Carbon Dioxide Spectroscopic Databank): updated and enlarged version for atmospheric applications. In: Proceedings of the 10th HITRAN database conference. Cambridge: MA, USA; 2008. [ftp://ftp.iao.ru/pub/CDSD-2008].
[21] Tashkun SA, Perevalov VI, Teffo JL, Bykov AD, Lavrentieva NN. CDSD-1000, the high-temperature carbon dioxide spectroscopic databank. J Quant Spectrosc Radiat Transf 2003;82:165–96.